

Gyromagnetic ratios and octupole collectivity in the structure of the $^{90-96}\text{Zr}$ isotopes

A. E. Stuchbery

Department of Nuclear Physics, Research School of Physical Sciences and Engineering, The Australian National University, Canberra, Australian Capital Territory 0200, Australia

N. Benczer-Koller and G. Kumbartzki

Department of Physics and Astronomy, Rutgers University, New Brunswick, New Jersey 08903, USA

T. J. Mertzimekis

National Superconducting Cyclotron Laboratory, Michigan State University, East Lansing, Michigan 48824, USA

(Received 15 December 2003; published 1 April 2004)

Shell model calculations have been performed for low-excitation states in the Zr isotopes between ^{90}Zr and ^{96}Zr with an emphasis on the g factors and electromagnetic decay rates for the lowest 2^+ and 3^- states. Overall the 2^+ states are reasonably well described. In contrast, the 3^- states present a puzzle because the measured g factors imply a single-particle configuration whereas the experimental $E3$ transition rates imply collective structures that cannot be explained by shell model calculations. A consistent description of the 3^- states in ^{90}Zr and ^{96}Zr is sought in terms of coupling between the single-particle structure and a collective octupole vibration.

DOI: 10.1103/PhysRevC.69.044302

PACS number(s): 21.10.Ky, 21.60.Cs, 27.70.+q, 21.10.Tg

I. INTRODUCTION

The g factors of low-excitation states in the even Zr isotopes from ^{90}Zr to ^{96}Zr have recently been measured by the transient-field technique in inverse kinematics [1–3] with the result that the data on magnetic moments in the $N=50$ region are now becoming quite extensive. Although there have been many shell model calculations on the Zr and Mo isotopes near $N=50$, most have not considered these observables, especially in nuclei with a few nucleons beyond $N=50$.

In the simplest single-particle model, the ground states of the Zr isotopes have a filled $\pi 2p_{1/2}$ subshell, and while the major neutron shell is closed at $N=50$ in ^{90}Zr , the $\nu 2d_{5/2}$ subshell is closed at $N=56$ in ^{96}Zr . Between ^{90}Zr and ^{96}Zr , the low-excitation structure is expected to be dominated by neutron $2d_{5/2}$ configurations.

Pioneering shell model calculations for the Zr isotopes were performed by Talmi and Unna [4], Auerbach and Talmi [5], and Vervier [6] in the 1960s. Model spaces with a few orbits outside $^{88}\text{Sr}_{50}$ or $^{90}\text{Zr}_{50}$ cores were considered. In the mid-1970s Gloeckner [7] determined effective interactions for the Zr and Nb isotopes with ^{88}Sr taken as an inert core and protons filling the $(2p_{1/2}, 1g_{9/2})$ levels and neutrons in the $(2d_{5/2}, 3s_{1/2})$ levels. There has been ongoing interest up to the present time. For example, recently Zhang *et al.* [8] studied nuclei with $N \geq 50$ and $A=92-98$ in the larger model space $\pi(1f_{5/2}, 2p_{3/2}, 2p_{1/2}, 1g_{9/2})$ and $\nu(1g_{9/2}, 2p_{1/2}, 2d_{5/2}, 3s_{1/2}, 2d_{3/2}, 1g_{7/2})$, and Holt *et al.* [9] considered the zirconium isotopes between ^{90}Zr and ^{100}Zr with a basis consisting of $\pi(2p_{1/2}, 1g_{9/2})$ and $\nu(2d_{5/2}, 3s_{1/2}, 2d_{3/2}, 1g_{7/2}, 1h_{11/2})$ and realistic effective interactions. Also recently, Johnstone and Towner calculated effective charges and effective magnetic dipole moments in the mass 90 region [10,11]. Lisetskiy *et al.* [12] performed shell model calculations for ^{94}Mo to investigate the nature of states assigned mixed symmetry in the proton-neutron inter-

acting boson model, and Werner *et al.* [13] extended the study to ^{95}Zr , including a consideration of the excited-state g factors.

The first part of the present study (in Secs. II and III) concerns shell model calculations of g factors in the Zr isotopes between ^{90}Zr and ^{96}Zr , performed using basis spaces and interactions that have previously been used to calculate the level sequences and transition rates [7,8]. While some aspects have been reported in Refs. [3,14,15], the focus here is on the g factors of the lowest 2^+ and 3^- states.

It has been recognized in the earlier work that the 2_1^+ -state g factors in the Zr and Mo isotopes with $N > 50$ may show evidence of collective features that are not easily accounted for in shell model calculations. Given that the measured $B(E3)$ for ^{96}Zr is among the strongest octupole-phonon to ground-state transitions observed in nuclei [16,17], by some measures stronger even than those found in ^{40}Ca and ^{208}Pb , it can be expected that collective features beyond the scope of limited-basis shell model calculations will also be important in relation to the 3_1^- states. After discussing the shell model calculations in Sec. III, which provide a benchmark against which the importance of collective components can be evaluated, it becomes evident that there is a dichotomy concerning single-particle and collective features of the 3^- states. As a first step towards the resolution of this dichotomy, the coupling of the single-particle configuration to the octupole vibration is considered by means of a semiempirical model in Sec. IV. Section V contains a summary and concluding remarks.

II. DETAILS OF THE SHELL MODEL CALCULATIONS

Shell model calculations were performed using the code OXBASH [18] for two different previously developed basis spaces, and their associated interactions, but with different levels of truncation.

TABLE I. Single-nucleon g factors near $Z=40$ and $N=50$.

Orbit	Theory ^a		Fit ^a		Present ^b
	$\pi 1p_{1/2}$ empty	$\pi 1p_{1/2}$ full	$\pi 1p_{1/2}$ empty	$\pi 1p_{1/2}$ full	
Protons					
$\pi 1f_{7/2}$					+1.456
$\pi 1f_{5/2}$					+0.544
$\pi 2p_{3/2}$	+1.621	+2.107			+2.063
$\pi 2p_{1/2}$	-0.260	-0.214			-0.063
$\pi 1g_{9/2}$	+1.388	+1.444	+1.358(7)	+1.438(9)	+1.354
Neutrons					
$\nu 2p_{1/2}$					+0.956
$\nu 1g_{9/2}$	-0.256	-0.268			-0.319
$\nu 2d_{5/2}$	-0.430	-0.508	-0.38(3)	-0.712(52)	-0.574
$\nu 3s_{1/2}$	-1.706	-2.190			-2.869
$\nu 2d_{3/2}$	+0.393	+0.479			+0.574
$\nu 2g_{7/2}$	+0.169	+0.208			+0.319
$\nu 1h_{11/2}$					-0.261

^aTheoretical effective g factors from Johnstone and Towner [11] and their empirical effective g factors determined from fits to nuclei with $N=50,51$.

^bSingle particle g factors used in the present study obtained by quenching the bare-nucleon spin g factors by a multiplicative factor of 0.75.

In the first set of calculations the basis space and interactions of Gloeckner [7] were applied. In these calculations the core is ^{88}Sr , with protons filling the $2p_{1/2}$ and $2g_{9/2}$ orbitals and neutrons filling the $2d_{5/2}$ and $3s_{1/2}$ orbitals. Following the terminology of the OXBASH program, this basis and its interactions are denoted “GL” in the following discussion. There is no need to restrict the orbital occupations in this basis, but it is limited in that no 3^- states can be formed in ^{90}Zr . On the other hand, this simple basis, with interactions from fits to the energy levels of nuclei near ^{88}Sr , gives a reasonably good account of most of the low-excitation

levels, including the 2_1^+ states (see below as well as Ref. [14] and references therein).

In the second case the more extended “GWB” basis was used with the “GWBXG” interactions, along the lines of recent calculations by Zhang *et al.* [8]. The GWBXG residual interaction combines effective interactions from the bare G matrix of the H7B potential [19] with empirically adjusted matrix elements and single-particle energies. Further details are provided in Ref. [8] and with the OXBASH online distribution [18]. The full basis space includes the $\pi(1f_{5/2}, 2p_{3/2}, 2p_{1/2}, 1g_{9/2})$ and $\nu(1g_{9/2}, 2p_{1/2},$

TABLE II. Shell model calculations of g factors of isomeric excited states and ground states in the Zr isotopes.

Isotope	J^π	E_x (keV)	Experiment ^a	Theory ^b		Configuration ^c
				GL	GWB	
^{90}Zr	5^-	2319	+1.25(3)	+1.213	+1.084	$\pi p_{1/2} g_{9/2}$
	8^+	3589	+1.356(7)	+1.355	+1.295	$\pi g_{9/2}^2$
^{91}Zr	$5/2^+$	0	-0.521448(1)	-0.557	-0.555	$\nu d_{5/2}$
	$15/2^-$	2288	+0.70(1)	+0.617	+0.594	$\pi p_{1/2} g_{9/2} \nu d_{5/2}$
	$21/2^+$	3167	+0.935(8)	+0.895	+0.868	$\pi g_{9/2}^2 \nu d_{5/2}$
^{95}Zr	$5/2^+$	0	(-0.452(8) ^d	-0.571	-0.573 ^e	$\nu d_{5/2}^5$

^aExperimental data from Refs. [23,24].

^bSee text for details of basis space and interactions. The large basis GWB calculations were not performed for ^{95}Zr .

^cMain configuration. For brevity fully occupied orbitals and empty orbitals, which do not contribute to the g factor, are not shown.

^dThe sign has not been measured but is assumed to be negative.

^eThe valence neutrons occupy only the $2d_{5/2}$ and $3s_{1/2}$ orbits in this calculation.

TABLE III. Shell model calculations of g factors, $B(E2)$'s, and excitation energies of 2_1^+ states in Zr isotopes. The energies are in keV and the $B(E2)$'s are in $e^2 \text{ fm}^4$. These shell model calculations have a closed neutron shell at $N=50$. The GWB basis calculations were performed with varying degrees of truncation in the neutron space: ds, only $2d_{5/2}$ and $3s_{1/2}$ are occupied; dsd, $2d_{5/2}$, $3s_{1/2}$, and $2d_{3/2}$ are occupied; dsdg, $2d_{5/2}$, $3s_{1/2}$, $2d_{3/2}$, and $1g_{7/2}$ are occupied (the full basis space). Since there are no valence neutrons beyond $N=50$ in ^{90}Zr the three calculations are (trivially) identical in that case. Data are from Refs. [1–3,25].

		Expt.	GL	GWB			Ref. [9]
				ds	dsd	dsdg	
^{90}Zr	E_x	2186	2228	2608	2608	2608	2003
	g	+1.25(21)	+1.355	+1.264	+1.264	+1.264	
	$B(E2; 2_1^+ \rightarrow 0_1^+)$	122(8)	55	33	33	33	45
^{92}Zr	E_x	934	878	807	942	979	581
	g	-0.180(10)	-0.444	-0.513	-0.409	-0.388	
	$B(E2; 2_1^+ \rightarrow 0_1^+)$	166(12)	138	138	155	165	73
^{94}Zr	E_x	919	855	744	904		520
	g	-0.329(15)	-0.537	-0.573	-0.329		
	$B(E2; 2_1^+ \rightarrow 0_1^+)$	132(28)	124	102	147		94
^{96}Zr	E_x	1750	1927	2643	2211		1426
	g	+0.03(7)	-0.082	-0.194	-0.142		
	$B(E2; 2_1^+ \rightarrow 0_1^+)$	110(44) ^a ; 61(15) ^b	144	127	164		22

^aReference [25].

^bReference [3].

$2d_{5/2}, 3s_{1/2}, 2d_{3/2}, 1g_{7/2}$) subshells, but for practical calculations there must be restrictions on the allowed configurations. In all calculations performed the proton excitations were constrained by the requirement that no more than two protons can be excited across the $Z=38$ subshell gap into $\pi 2p_{1/2}$ and $\pi 1g_{9/2}$. Particle-hole excitations across the $N=50$ neutron shell closure were not allowed, except in some supplementary calculations discussed in Sec. III B. In $^{91,92}\text{Zr}$, the occupation of the $2d_{5/2}$, $3s_{1/2}$, $2d_{3/2}$, and $1g_{7/2}$ orbits by the two valence neutrons can be unrestricted; however, for the heavier isotopes it is necessary that restrictions be placed on the occupation of these orbits. As far as the first 2^+ states are concerned, the lowest two neutron orbits, namely, $2d_{5/2}$ and $3s_{1/2}$, are expected to be most important. This expectation was tested by a series of calculations in the GWB basis with varying levels of truncation.

The effective charges of the proton and neutron were taken to be $e_{\pi}^{\text{eff}}=1.77$ and $e_{\nu}^{\text{eff}}=1.19$, consistent with values suggested in Refs. [7,9,10] for the $E2$ effective charges. There is no *a priori* reason to expect the same effective charges for the $E3$ operator. However, in the regions of strong octupole collectivity around ^{146}Gd and ^{208}Pb the $E3$ effective charges resemble those assumed here for the $E2$ operator once octupole-vibration coupling is explicitly taken into account [20,21]. As a first approximation it will be assumed that the $E2$ and $E3$ effective charges are the same. A shortfall in the calculated $E3$ transition rates will be interpreted as evidence of octupole phonon admixtures. A similar approach has been taken in recent shell model calculations near ^{100}Sn [22].

The intrinsic spin g factors of the nucleons were quenched to 0.75 times the bare nucleon values, i.e., $g_s(\pi)=+4.19$, $g_s(\nu)=-2.87$, while the orbital g factors were $g_l=1(0)$ for

protons (neutrons). A similar quenching factor of 0.7 was used in Ref. [13]. In Table I the resulting single-nucleon g factors of interest for the following discussion are compared with theoretical and experimental effective g factors obtained by Johnstone and Towner [11]. These authors have identified a significant difference in effective single-particle g factors depending on the orbit and on whether the $2\pi p_{1/2}$ orbit is empty or full. They also fitted data for $N=50$ and $N=51$ to determine experimental effective g factors for the $\pi 1g_{9/2}$ and $\nu 2d_{5/2}$ orbits upon which the present calculations depend most sensitively. The g factors adopted for the calculations below agree within the experimental limits with those obtained by Johnstone and Towner, and also give a reasonably good description of the states with relatively pure configurations discussed in the following section.

III. RESULTS AND DISCUSSION OF SHELL MODEL CALCULATIONS

A. g factors of ground-states and high-spin isomers

Table II compares the experimental and theoretical g factors for the high-spin isomers and ground states of the odd- A isotopes ^{91}Zr and ^{95}Zr (see also Ref. [14]). On the whole the g factors of these states are well reproduced and the configuration designated in the last column of Table II is dominant in the wave function. These relatively simple states provide a point of comparison for the 2^+ and 3^- states considered in the following subsections.

Although the g factors appear to be better described by the calculations with the simpler GL basis, this improvement is an artifact of the choice of quenching factors for the bare-nucleon spin g factors. It would be reasonable to use spin g

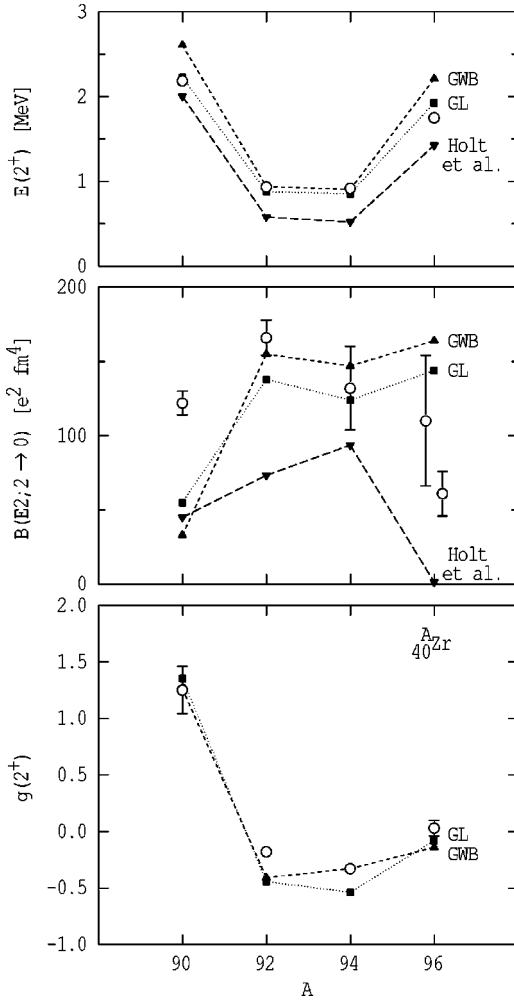


FIG. 1. Comparisons between the present shell model calculations, those of Holt *et al.* [9], and experiment. Experimental data are designated by the open circles. The results shown for the GWB basis are those for the “dsd” truncation.

factors that are closer to the bare-nucleon values in the larger-basis calculations and thereby bring theory and experiment into better agreement, but such fine tuning has not been pursued here.

B. Properties of the 2_1^+ states

Table III compares theory and experiment for the excitation energy, $B(E2; 2_1^+ \rightarrow 0_1^+)$, and g factor of the 2_1^+ states in $^{90,92,94,96}\text{Zr}$. The present shell model calculations are also compared with experiment and the results of recent calculations [9] in Fig. 1. Overall the main trends in the data are reproduced by the calculations. The $B(E2)$ values obtained in the GL and GWB calculations are in reasonable agreement with each other, and for $^{92,94,96}\text{Zr}$ the agreement with experiment is reasonably good, and possibly better than that in the calculations of Holt *et al.* [9].

For ^{90}Zr , both the present calculations and those of Holt *et al.* underestimate the observed transition rate. Since these calculations have a closed $N=50$ shell, further calculations (not shown in Table III) which allowed neutrons to excite

across the $N=50$ shell gap, were performed in the GWB basis. In the first place, excitations from the $\nu p_{1/2}$ orbit alone were allowed. It was found that the calculated transition rate increased by about 25%, but there was little effect on the g factor. A neutron hole was then allowed in either the $\nu p_{1/2}$ or the $\nu g_{9/2}$ orbit. With this larger configuration space the transition rate increased to $174 e^2 \text{fm}^4$, which is larger than experiment. At first sight an experimental $2_1^+ \rightarrow 0_1^+$ transition rate that is larger than a shell model calculation might be associated with increased quadrupole collectivity in the 2_1^+ state. However, in these calculations for ^{90}Zr , the changes in the $E2$ transition rate are predominantly due to a redistribution of the amplitudes in the ground-state wavefunction, while the structure of the 2_1^+ state is relatively little affected, as is evidenced by the calculated $g(2_1^+)$ value which is reduced only a little, from 1.264 to 1.156. Thus the comparison of the experimental and theoretical $B(E2)$ values for ^{90}Zr in Table III cannot be taken as an unambiguous signature of extra collectivity in the 2_1^+ state since it can also be explained if the theoretical wave function of the ground state is modified somewhat.

With the possible exception of ^{96}Zr , the larger basis GWB calculations give improved g factor values for the 2_1^+ states. In ^{90}Zr the 2_1^+ state is predominantly $\pi(g_{9/2})_{2^+}^2$, whereas in ^{92}Zr and ^{94}Zr the 2_1^+ states are predominantly neutron excitations, $\nu(d_{5/2})_{2^+}^2$ and $\nu(d_{5/2})_{2^+}^4$, respectively. These conclusions hold for calculations in both basis spaces and for all levels of truncation of the GWB basis. Note that the transition rate increases and the g factor decreases as the number of orbits included in the GWB calculation is increased, generally bringing both into better agreement with experiment.

A feature of the level spectra of the even Zr and Mo isotopes near $N=50$ that has been emphasized recently [8,9,14] is the apparent weak coupling of the proton and neutron valence spaces. This phenomenon gives rise to predicted 2_1^+ states in the $N=52,54$ nuclei $^{92,94}\text{Zr}$ and $^{94,96}\text{Mo}$ that are predominantly $\nu(d_{5/2})^n$ excitations. As discussed in Ref. [14], it cannot be judged from the level spectrum alone whether the proton-neutron (pn) coupling is weak or rather strong and state independent. Magnetic moments, however, can probe the proton-neutron coupling through their sensitivity to the relative contributions of protons and neutrons to the angular momentum of the states. Indeed, the g factor data were used by Werner *et al.* [13] to adjust the strength of the $T=0$ channel of the pn interaction in their shell model calculations for ^{92}Zr . It is beyond the scope of the present study to seek an optimal basis space and set of effective interactions for the Zr isotopes. Although better agreement could be achieved by further tuning the interactions, the moment data generally support the weak-coupling picture as a first approximation, and show that it is more appropriate in the Zr isotopes than in the Mo isotopes.

Because the $\nu 2d_{5/2}$ subshell is filled in the ground state of ^{96}Zr , the structure of its 2_1^+ state becomes much more complex. It arises from a competition between many terms, including $\pi(g_{9/2})_{2^+}^2$, $\nu(d_{5/2}^5 s_{1/2})_{2^+}$, and $\nu(d_{5/2}^5 d_{3/2})_{2^+}$. The wave function is very different for the GL and GWB calculations:

$$|\phi(2_1^+)\rangle_{\text{GL}} = 36\% |\pi g_{9/2}^2 \nu d_{5/2}^4 s_{1/2}^2\rangle + 29\% |\nu d_{5/2}^5 s_{1/2}\rangle + 25\% |\pi g_{9/2}^2 \nu d_{5/2}^5 s_{1/2}\rangle + \dots, \quad (1)$$

TABLE IV. Shell model calculations of g factors $B(E3)$'s and excitation energies of 3_1^- states in Zr isotopes. These calculations have closed $N=50$ shell. The energies are in keV and the $B(E3)$ values are in $e^2 \text{ fm}^6$. Data are from Refs. [2,16,17].

		Expt.	GL			GWB	
				ds	dsd	dsdg	
^{90}Zr	E_x	2748		3190	3190	3190	
	g	+0.986(56)		+1.124	+1.124	+1.124	
	$B(E3; 3_1^- \rightarrow 0_1^+)$	$[14.0(7)] \times 10^3$		2725	2725	2725	
^{92}Zr	E_x	2340	2943	2981	2996	3007	
	g		+1.787	+1.282	+1.247	+1.238	
	$B(E3; 3_1^- \rightarrow 0_1^+)$	$[10(3)] \times 10^3$	0	2932	3044	3036	
^{94}Zr	E_x	2058	3043	3250	3199		
	g		+2.034	+1.336	1.285		
	$B(E3; 3_1^- \rightarrow 0_1^+)$	$[13(4)] \times 10^3$	0	3180	3214		
^{96}Zr	E_x	1897	3906	4137	3913		
	g	+0.96(17)	+1.899	+1.177	+1.175		
	$B(E3; 3_1^- \rightarrow 0_1^+)$	$[26(3)] \times 10^3$	0	5030	4601		

$$|\phi(2^+)_{\text{GWB}} = 45\% | \nu d_{5/2}^5 d_{3/2} \rangle + 11\% | \nu d_{5/2}^5 s_{1/2} \rangle + 4\% | \pi g_{9/2}^2 \nu d_{5/2}^5 d_{3/2} \rangle + \dots \quad (2)$$

Experimentally, the g factor is near zero and favors a positive sign, but within two standard deviations of the experimental uncertainties, $-0.11 < g < +0.17$, a negative sign is also possible. The GL calculation comes within this range, while the GWB result is slightly outside of it. Despite the rather different wave functions, the $B(E2)$ values obtained in the two calculations are in reasonable agreement with each other and within a factor of 2 to 3 of experiment. The 2_1^+ state in ^{96}Zr evidently results from a balance between proton and neutron excitations. Although the wave function is spread over a number of configurations, the state is far from collective. Further work on the basis space and residual interactions applicable for ^{96}Zr is needed to improve the 2^+ state g factor calculation.

It has been noted previously that the experimental g factors of 2^+ states near closed shells are displaced somewhat from the shell model values in the direction of the collective estimate, Z/A (≈ 0.43 for the Zr isotopes under consideration), which suggests extra collective components in the 2_1^+ -state wave functions that are not included in the shell model calculations [14,15,26–28]. The present results for $^{92,94,96}\text{Zr}$ also show this trend. There may be scope for further investigations of the 2_1^+ states in the Zr isotopes between ^{90}Zr and ^{96}Zr along the lines of those presented for ^{44}Ca in Ref. [29], in which the 2^+ state is written as a superposition of a collective component and a single-particle component. (See also the analysis of the 3_1^- states presented below.) However, this type of analysis was not pursued here because the main trends in the data concerning the 2_1^+ states are reproduced by the shell model approach (see Fig. 1) and it would be appropriate to refine the shell-model interactions, and effective charges, before reverting to a semiempirical particle-vibration coupling analysis of these 2^+ states. Furthermore,

$B(E2)$ systematics [25] reveal that the $^{90-96}\text{Zr}$ isotopes form one of the regions of lowest quadrupole collectivity in the nuclear chart. Taking this observation together with the fact that the shell model $B(E2)$'s are already close to experiment strongly suggests that a particle-vibration analysis of the 2_1^+ states would be inappropriate.

C. Properties of the 3_1^- states

While the overall trends in the excitation energies, $B(E2)$'s, and g factors of the 2_1^+ states are reasonably well reproduced by the shell model calculations, clear disparities in the energy trends and $B(E3)$ values are apparent in the calculations for the 3^- states, as shown in Table IV and Fig. 2. In ^{90}Zr , the excitation energy and g factor are quite well reproduced by the GWB calculation (all columns under GWB in the table are the same because $N=50$ is closed). However, the $B(E3)$ is underestimated by a factor of 5. According to the shell model calculations, which are supported by the experimental g factor, the 3^- state in ^{90}Zr is mainly due to the $\pi(p_{3/2}g_{9/2})_{3^-}$ configuration. The full transition strength for a pure $\pi(p_{3/2}g_{9/2})_{3^-} \rightarrow \pi(p_{3/2})_{0_1^+}$ transition would be $\sim 7100 e^2 \text{ fm}^6$, which is still only half of the experimental value. Thus the shortfall in the $B(E3)$ value cannot be ascribed to the properties of the ground-state wave function as discussed above in relation to the $B(E2; 2_1^+ \rightarrow 0_1^+)$ value in ^{90}Zr . Instead, this observation strongly suggests that there are collective octupole contributions in the 3^- state that the shell model with a closed $N=50$ shell does not include. The relatively good agreement between the experimental g factor and that of a pure $\pi(p_{3/2}g_{9/2})$ configuration may be partly fortuitous: It can be seen from the g factors of the configurations near the Fermi surface, listed in Table V, that the $\pi(p_{3/2}g_{9/2})_{3^-}$ configuration has a g factor of intermediate magnitude compared with the other 3^- configurations near the Fermi surface. If these other proton and neutron configurations are present in the 3^- wave function, their contribu-

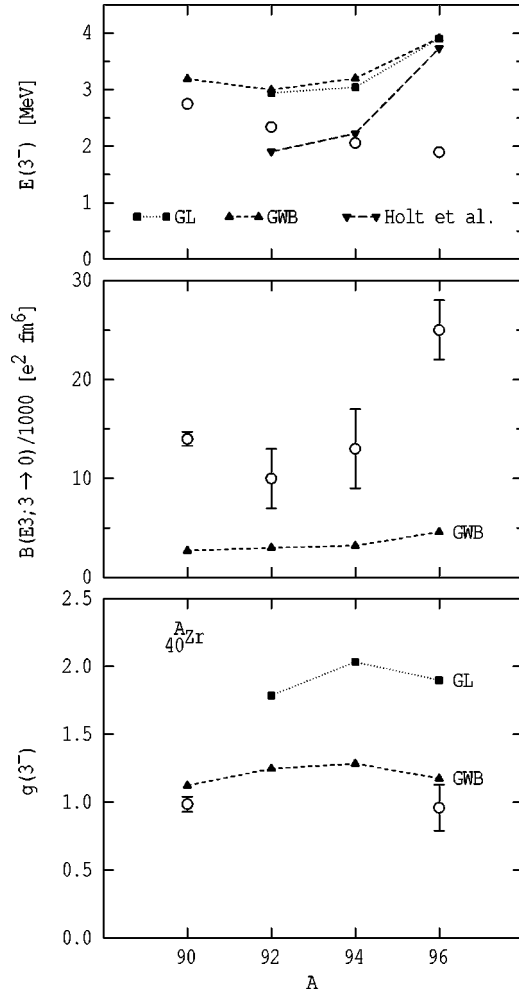


FIG. 2. Comparisons between the present shell model calculations, those of Holt *et al.* [9], and experiment. Experimental data are designated by the open circles. The results shown for the GWB basis are those for the “dsd” truncation. The $B(E3)$ is zero for all cases in the GL basis, and is small in the basis employed by Holt *et al.* [9]; see text.

tions to the g factor might largely cancel and result in a somewhat collective 3^- state with a g factor close to that of the dominant single-particle configuration. This conjecture is in accord with the particle-vibration analysis in the following section.

As neutrons are added to ^{90}Zr , the excitation energy of the experimental 3^- state decreases with each additional pair of neutrons. (See Fig. 2.) In the GWB shell model, there is a decrease between ^{90}Zr and ^{92}Zr , but only half of the magnitude of that observed experimentally. Thereafter, the shell model calculations predict that the 3^- state energy increases with the addition of neutron pairs, to the point where in ^{96}Zr , the experimental and theoretical excitation energies differ by 2 MeV, with the calculated level at over twice the excitation energy of the observed level. It is relevant to note that similar trends were found in the shell model calculations of Holt *et al.* [9]. In their calculations, and for the GL basis, the 3^- states are primarily due to the configurations $[\pi(p_{1/2}g_{9/2})_{4-} \otimes \nu(d_{5/2})_{2+}^2]_{3-}$ and $[\pi(p_{1/2}g_{9/2})_{5-} \otimes \nu(d_{5/2})_{2+}^2]_{3-}$. These con-

TABLE V. g factors of low-excitation 3^- configurations.

Configuration	g factor
$\pi(f_{5/2}g_{9/2})_{3-}$	+1.489
$\pi(f_{7/2}g_{9/2})_{3-}$	+1.367
$\pi(p_{3/2}g_{9/2})_{3-}$	+1.088
$\nu(p_{1/2}d_{5/2})_{3-}$	-0.319
$\nu(p_{1/2}g_{7/2})_{3-}$	+0.239
$\nu(d_{5/2}h_{11/2})_{3-}$	-0.065
$\nu(g_{9/2}h_{11/2})_{3-}$	-0.263
$[\pi(p_{1/2}g_{9/2})_{4-} \otimes \nu(d_{5/2})_{2+}^2]_{3-}$	+1.669
$[\pi(p_{1/2}g_{9/2})_{5-} \otimes \nu(d_{5/2})_{2+}^2]_{3-}$	+2.015
$[\pi(p_{1/2}g_{9/2})_{4-} \otimes \nu(d_{5/2}s_{1/2})_{2+}]_{3-}$	+1.637
$[\pi(p_{1/2}g_{9/2})_{5-} \otimes \nu(d_{5/2}s_{1/2})_{2+}]_{3-}$	+1.914

figurations have g factors that are significantly larger than experiment (Table V). Furthermore, in contrast with the strong $E3$ transitions observed experimentally, there is no one-body transition strength to connect these configurations to the ground state. For calculations in the GWB basis, the octupole transitions in all isotopes stem from the proton $g_{9/2} \rightarrow p_{3/2}$ transition. The increased theoretical value for ^{96}Zr (Table IV) is due primarily to changes in the ground-state wave function that are associated with the $d_{5/2}$ subshell closure, not to a change in the structure of the 3^- state. In fact the experimental g factor, as well as the GWB shell model calculation, imply that the 3^- state wave function is dominated by the $\pi(p_{3/2}g_{9/2})$ configuration, very much like the 3^- state in ^{90}Zr .

The shell model calculations of the $B(E3)$ transition rates could be brought into agreement with experiment by using an effective charge for the proton of $e_{\pi}^{\text{eff}} \sim 4$. The description of ^{90}Zr would then be quite good, but the calculated excitation energies in the heavier isotopes would remain problematic.

Thus the present shell model calculations imply that proton single-particle configurations are dominant in the 3^- state wave functions of all four Zr isotopes, but put the excitation energies too high and fail to account for the strong $E3$ transitions to the ground states (on average by a factor of ~ 5). As mentioned above, the measured $B(E3)$ for ^{96}Zr is one of the strongest octupole-phonon to ground-state transitions observed in nuclei (see, e.g., Refs. [16,17] and references therein). The 3^- states therefore present a puzzle, especially in ^{96}Zr , where the state is apparently strongly collective and yet the experimental g factor clearly shows single-proton characteristics that are expected to be lost in a collective state. Although the implications of the experimental g factor and the measured lifetime seem contradictory, it is difficult to believe that either measurement is incorrect. The following section therefore presents a semiempirical particle-vibration coupling analysis (cf. Ref. [30]) that seeks a consistent explanation of the measured g factors and $E3$ transition rates in ^{90}Zr and ^{96}Zr . It is motivated in part by the observation that an effective proton charge of $e_{\pi}^{\text{eff}} \sim 4$, which would be required to bring the shell model calculations into harmony with experiment, is similar in magnitude to those found for

$E3$ transitions between the “single-particle” states in the ^{208}Pb region where the coupling of the single-particle states to the octupole vibration has been well studied (see Ref. [31], Table 6-15, p. 564).

IV. PARTICLE-VIBRATION COUPLING AND THE 3^- STATES

Octupole collectivity is associated with regions of the nuclear shell model where there are single particle orbits with $\Delta l=3$ and $\Delta j=3$ available near the Fermi surface for both protons and neutrons. The most relevant configurations for 3^- states in the Zr isotopes are $\pi(p_{3/2}g_{9/2})$ and $\nu(d_{5/2}h_{11/2})$. Strong octupole correlations are expected because these orbits for both protons and neutrons are separated by a similar energy, about 3.5 to 4 MeV.

Coupling between the octupole mode and a single-particle configuration gives rise to “renormalized” single-particle states containing significant octupole-coupled admixtures (see, for example, Ref. [31], pp. 562–566). Thus the observed octupole-coupled $\pi\tilde{g}_{9/2}$ state in the Zr region would be represented as

$$|\tilde{g}_{9/2}\rangle = \zeta|g_{9/2}\rangle + \sqrt{1-\zeta^2}|(p_{3/2} \otimes 3^-_{\text{coll}})_{9/2}\rangle, \quad (3)$$

where 3^-_{coll} represents the collective octupole vibration and the tilde indicates that the empirical single-particle state includes octupole-coupled components. As another example, a (d,p) experiment on ^{89}Sr [32] reports an admixture of the $11/2^-$ member of the $\nu d_{5/2} \otimes 3^-$ multiplet with the $\nu h_{11/2}$ orbital, where 3^- corresponds to the core excitation in ^{88}Sr .

As a first approximation in which Pauli blocking effects are ignored, it is reasonable to write the wave functions of the predominantly $\pi(p_{3/2}g_{9/2})$ 3^-_1 states in ^{90}Zr and ^{96}Zr in the form

$$|3^-_1\rangle = \alpha|3^-_{\text{coll}}\rangle + \sqrt{1-\alpha^2}|3^-_{\text{shell}}\rangle, \quad (4)$$

where $|3^-_{\text{shell}}\rangle$ represents the shell model configuration, and the mixing amplitude $\alpha < 1$. In other words it will be assumed, as a first approximation, that the internal structure of the collective 3^- state is changed little by coupling it to a particular shell model configuration. This assumption may not be entirely justified. Despite this caveat an attempt will be made to apply a simple particle-vibration model as a feasibility estimate, i.e., to give an indication whether a more sophisticated particle-vibration approach might possibly explain both the “single-particle” g factors and the “collective” $E3$ decay strengths of the 3^-_1 states in ^{90}Zr and ^{96}Zr .

It follows from Eq. (4) that the observed g factor and $B(E3)$ are given by

$$g(3^-_1) = \alpha^2 g_{\text{coll}} + (1-\alpha^2)g_{\text{shell}} \quad (5)$$

and

$$B(E3) = \alpha B(E3)_{\text{coll}} \pm \sqrt{1-\alpha^2} B(E3)_{\text{shell}}, \quad (6)$$

where the subscripts “coll” and “shell” indicate the collective and shell model contributions, respectively. In a purely em-

pirical model there is a sign ambiguity in the expression for the $B(E3)$. Fortunately, however, the effect of this uncertainty in the sign is mitigated because $B(E3)_{\text{coll}} \gg B(E3)_{\text{shell}}$. To proceed, in the spirit of obtaining a credibility estimate for this type of approach, the following analysis assumes the most optimistic alternative, namely, a positive sign in Eq. (6). The effect of taking the negative sign will be discussed toward the end of the section.

Since $\alpha < 1$, and $g_{\text{coll}} \ll g_{\text{shell}}$, while $B(E3)_{\text{coll}} \gg B(E3)_{\text{shell}}$, Eqs. (5) and (6) indicate that the $B(E3)$ can be much more sensitive to small collective admixtures than the g factor, which suggests that an appropriately mixed state might show both a g factor near the single-particle value and a collective $E3$ transition strength to the ground state.

A consistent description of the g factor and $B(E3)$ data for the 3^-_1 states in ^{90}Zr and ^{96}Zr was sought using Eqs. (4)–(6). There are two experimental g factors and two experimental $B(E3)$ values to be explained, making four experimental data in all. If the constituent g factor and $B(E3)$ values, as well as the mixing amplitudes, on the right-hand sides of Eqs. (5) and (6) are treated as unknowns there can be up to ten free parameters. To make a meaningful analysis, as many of these variables as possible should be fixed to independently determined theoretical or experimental values. In this semiempirical approach the mixing amplitudes, α_{90} and α_{96} for ^{90}Zr and ^{96}Zr , respectively, are free parameters, which leaves scope for one, or at most two, other free parameters.

The analysis which follows uses only a single free parameter to prescribe the $B(E3)_{\text{coll}}$ values in both ^{90}Zr and ^{96}Zr . The remaining parameters, g_{coll} , g_{shell} , and $B(E3)_{\text{shell}}$ are fixed. The shell model g factors and $B(E3)$ values for ^{90}Zr and ^{96}Zr were taken from the results in the penultimate column of Table IV. The value $g_{\text{coll}}=0.55$ was assumed for both ^{90}Zr and ^{96}Zr based on previous theoretical work and comparisons with experimental g factors of well known collective vibrational states. Collective vibrational states may be modeled using the random phase approximation (RPA) or its extension the quasiparticle random phase approximation (QRPA). Such calculations by Rosso *et al.* [33] for ^{96}Zr imply that the lowest collective 3^- state has a wave function dominated by the $\pi(p_{3/2}^{-1}g_{9/2})$ and $\nu(d_{5/2}^{-1}h_{11/2})$ configurations, which have about equal weight, with smaller contributions from many other configurations including $\pi(f_{7/2}^{-1}g_{9/2})_{3^-}$ and $\nu(g_{9/2}^{-1}h_{11/2})_{3^-}$, for example. Unfortunately g factors were not evaluated. However, based on the RPA and QRPA wave functions tabulated in Ref. [33] (which list only the dominant terms), and the corresponding g factor values listed in Table V, it is reasonable to estimate that $g(3^-_1)$ for the lowest collective octupole state in ^{96}Zr , is similar in magnitude to the g factors of the octupole vibrational states in ^{16}O , ^{40}Ca , and ^{208}Pb , all of which have experimental g factors between ~ 0.5 and ~ 0.6 . Thus the following evaluations use $g_{\text{coll}}=0.55$ for both ^{90}Zr and ^{96}Zr .

It remains to specify the collective component of the $B(E3)$. In the absence of a clearly applicable theoretical value, $B(E3)_{\text{coll}}$ was parametrized by making use of the form of the $E3$ sum rule in the hydrodynamical model with irrotational flow (Ref. [31], p. 405), i.e.,

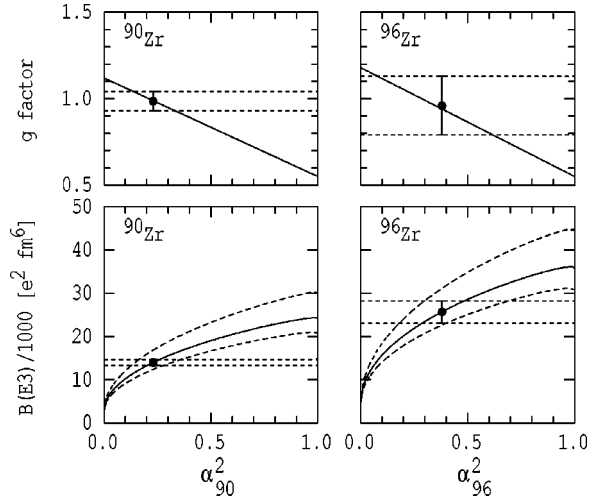


FIG. 3. Empirical particle-vibration coupling model analysis of the $g(3^-)$ and $B(E3;3^- \rightarrow 0^+)$ values in ^{90}Zr and ^{96}Zr . In the lower panels the solid lines represent the theory for the best fit value of the parameter C while the dashed lines indicate the uncertainty in the calculated $B(E3)$ due to the uncertainty in C .

$$E^n B(E3) = CZ^2 A^{1/3}, \quad (7)$$

where C is a constant and the classical harmonic oscillator model has the excitation energy of the 3^- state, E , raised to the power $n=1$ [31]. In previous work C and n have been treated as free parameters to fit $E3$ systematics [16,34]. Here C alone was treated as a free parameter (with $n=1$) to set the $B(E3)_{\text{coll}}$ values in ^{90}Zr and ^{96}Zr . Thus a simultaneous fit to the g factors and $B(E3)$ values was sought with three parameters: C , α_{90} , and α_{96} .

The results are presented in Fig. 3, where the theoretical g and $B(E3)$ values are plotted as a function of the collective amplitudes (α^2) in the 3^- wave functions. The theoretical $B(E3)$ values are plotted for the fitted value of $C = 65_{-9}^{+16}$ MeV e^2 fm 6 , and the experimental data are plotted at the α^2 values corresponding to $C=65$, where the chi-square has its minimum value. [According to conventional usage, the value of C corresponds to using $B(E3;0^+ \rightarrow 3^-) = 7B(E3;3^- \rightarrow 0^+)$ in Eq. (7). The error limits were obtained assuming no uncertainties in the theoretical parameters.] Clearly, the experimental g factors and $B(E3)$ values in ^{90}Zr and ^{96}Zr can be reproduced using Eqs. (4)–(7) with a single value of C . As expected, a greater collective component is required in ^{96}Zr than in ^{90}Zr but, more surprisingly, for the best-fit value of C , the 3^- states remain predominantly single-particle excitations in both ^{90}Zr and ^{96}Zr . At the lower limit of the C values allowed by the experimental errors on the g factor and $E3$ data, the ^{90}Zr 3^- state is 70 % single particle while the ^{96}Zr state is 50 % single-particle structure and 50 % collective.

It can be concluded that a consistent explanation of the g factors and $E3$ transition rates is possible in terms of a semi-empirical particle-vibration coupling analysis. However, the plausibility of this analysis depends on whether the implied $B(E3)_{\text{coll}}$ values are reasonable or not—a point that is sharp-

ened because $B(E3)_{\text{coll}}$ must exceed the experimental $B(E3;3^- \rightarrow 0^+)$ in magnitude, and the experimental $B(E3;3^- \rightarrow 0^+)$ in ^{96}Zr is already exceptionally strong [16]. The $B(E3)_{\text{coll}}$ values appear at $\alpha^2=1$ in Fig. 3: in ^{90}Zr $B(E3)_{\text{coll}}$ is of the same magnitude as the measured $B(E3;3^- \rightarrow 0^+)$ in ^{96}Zr , which seems reasonable, and while $B(E3)_{\text{coll}}$ is 39 $^{+37}_{-24}$ % stronger than the measured $B(E3;3^- \rightarrow 0^+)$ in ^{96}Zr , this too does not appear to be unreasonably strong. In fact the implied magnitude of $B(E3)_{\text{coll}}$ in ^{96}Zr is consistent with some of the earlier experimental data [17], in which the octupole collectivity was about 40% stronger than the more recent (and more reliable) experimental value reported by Horen *et al.* [16], which is adopted in the present work.

The discussion in the preceding paragraphs, and the results presented in Fig. 3, correspond to taking the positive sign in Eq. (6). If the negative sign is used instead, the main change is that the best-fit value of C increases to $C = 94 \pm 19$ MeV e^2 fm 6 while the mixing amplitudes for the best fit are almost unchanged. The C values obtained for the two alternate signs in Eq. (6) overlap within their assigned errors. For the positive sign the required $B(E3)_{\text{coll}}$ values in both ^{90}Zr and ^{96}Zr exhaust about (12 \pm 2)% of the energy-weighted sum rule; for the negative sign the $B(E3)_{\text{coll}}$ values exhaust about (18 \pm 4)% of the energy-weighted sum rule [31,35]. Although the data are more readily explained if the positive sign applies, the model parameters remain within the realm of credibility for a negative sign as well.

Thus it can be concluded that a consistent, empirical explanation of the g factors and $E3$ transition rates is possible with reasonable parameters. To place this empirical particle-vibration approach on a more rigorous microscopic footing, however, is a matter for future investigations. For example, sufficiently large basis shell model calculations that include the important $\pi(p_{3/2}g_{9/2})$ and $\nu(d_{5/2}h_{11/2})$ configurations would be valuable.

V. SUMMARY AND CONCLUSION

The properties of the first 2^+ and 3^- states in the even Zr isotopes between ^{90}Zr and ^{96}Zr have been examined in the shell model and compared with experimental data, especially recent g factor results [1–3]. Generally the description of the 2^+ states is satisfactory.

The 3^- states are more enigmatic. The agreement between shell model theory and experiment is good for the g factors in ^{90}Zr and ^{96}Zr , implying a state dominated by the proton configuration $\pi(p_{3/2}g_{9/2})_{3^-}$. Despite this apparent single-particle structure, the $E3$ transition strength observed in both nuclei is a factor of 5 larger than the shell model calculations predict, which seems to imply that the first 3^- states are collective, and strongly so in ^{96}Zr .

It has been demonstrated that the dichotomy concerning the 3^- states can be resolved in terms of an empirical particle-vibration approach, which introduces a collective contribution into the wave functions of otherwise single-

particle states. The success of this simple empirical approach invites further investigation to illuminate its microscopic basis.

The experimental g factors and the present analysis make it very clear that there remain strong single-particle components in the otherwise apparently collective 3_1^- states of ^{90}Zr and ^{96}Zr , a feature that would hardly have been anticipated without the g factor data.

ACKNOWLEDGMENTS

A portion of this work was completed while the first author was on sabbatical leave at the National Superconducting Cyclotron Laboratory (NSCL), Michigan State University. It was supported in part by NSF Grant Nos. PHY01-10253 and PHY99-83810. The authors are grateful to several colleagues, especially Dr. E. Stefanova, for helpful comments on the text.

-
- [1] G. Jakob, N. Benczer-Koller, J. Holden, G. Kumbartzki, T. J. Mertzimekis, K.-H. Speidel, C. W. Beausang, and R. Krücken, *Phys. Lett. B* **468**, 13 (1999).
- [2] G. Jakob, N. Benczer-Koller, J. Holden, G. Kumbartzki, T. J. Mertzimekis, K.-H. Speidel, R. Ernst, P. Maier-Komor, C. W. Beausang, and R. Krücken, *Phys. Lett. B* **494**, 187 (2000).
- [3] G. Kumbartzki, N. Benczer-Koller, J. Holden, G. Jakob, T. J. Mertzimekis, M. J. Taylor, K.-H. Speidel, R. Ernst, P. Maier-Komor, A. E. Stuchbery, C. W. Beausang, and R. Krücken, *Phys. Lett. B* **562**, 193 (2003).
- [4] I. Talmi and I. Unna, *Nucl. Phys.* **19**, 225 (1960).
- [5] N. Auerbach and I. Talmi, *Nucl. Phys.* **64**, 458 (1965).
- [6] J. Vervier, *Nucl. Phys.* **75**, 17 (1966).
- [7] D. H. Gloeckner, *Nucl. Phys.* **A253**, 301 (1975).
- [8] Chang-hua Zhang, Shun-jin Wang, and Jin-nan Gu, *Phys. Rev. C* **60**, 054316 (1999).
- [9] A. Holt, T. England, M. Hjorth-Jensen, and E. Osnes, *Phys. Rev. C* **61**, 064318 (2000).
- [10] I. P. Johnstone and I. S. Towner, *Eur. Phys. J. A* **2**, 263 (1998).
- [11] I. P. Johnstone and I. S. Towner, *Eur. Phys. J. A* **3**, 237 (1998).
- [12] A. F. Lisetskiy, N. Pietralla, C. Fransen, R. V. Jolos, and P. von Brentano, *Nucl. Phys.* **A677**, 100 (2000).
- [13] V. Werner, D. Belic, P. von Brentano, C. Fransen, A. Gade, H. von Garrel, J. Jolie, U. Kneissl, C. Kohstall, A. Linnemann, A. F. Lisetskiy, N. Pietralla, H. H. Pitz, M. Scheck, K.-H. Speidel, F. Stedile, and S. W. Yates, *Phys. Lett. B* **550**, 140 (2002).
- [14] P. F. Mantica, A. E. Stuchbery, D. E. Groh, J. I. Prisciandaro, and M. P. Robinson, *Phys. Rev. C* **63**, 034312 (2001).
- [15] A. E. Stuchbery, *Nucl. Phys.* **A682**, 470 (2001).
- [16] D. J. Horen, R. L. Auble, G. R. Satchler, J. R. Beene, I. Y. Lee, C. Y. Wu, D. Cline, M. Devlin, R. Ibbotson, and M. W. Simon, *Phys. Rev. C* **48**, R2131 (1993).
- [17] T. Kibedi and R. H. Spear, *At. Data Nucl. Data Tables* **80**, 35 (2002).
- [18] A. Etchegoyen, W. D. Rae, N. S. Godwin, W. A. Richter, C. H. Zimmerman, B. A. Brown, W. E. Ormand, and J. S. Winfield, MSU-NSCL Report No. 524, 1985 (unpublished).
- [19] A. Hosaka, K. I. Kubo, and H. Toki, *Nucl. Phys.* **A444**, 76 (1985).
- [20] M. Piiparinen, P. Kleinheinz, S. Lunardi, M. Ogawa, G. de Angelis, F. Soramel, W. Meczynskiand, and J. Blomqvist, *Z. Phys. A* **337**, 387 (1990).
- [21] M. Rejmund, K. H. Maier, R. Broda, B. Fornal, M. Lach, J. Wrzesinski, J. Blomqvist, A. Gadea, J. Gerl, M. Górska, H. Grawe, M. Kaspar, H. Schaffner, Ch. Schlegel, R. Schubart, and H. J. Wollersheim, *Eur. Phys. J. A* **8**, 161 (2000).
- [22] M. Górska, H. Grawe, D. Kast, G. de Angelis, P. G. Bizzeti, B. A. Brown, A. Dewald, C. Fahlander, A. Gadea, A. Jungclaus, K. P. Lieb, K. H. Maier, D. R. Napoli, Q. Pan, R. Peusquens, M. De Poli, M. Rejmund, and H. Tiesler, *Phys. Rev. C* **58**, 108 (1998).
- [23] P. Raghavan, *At. Data Nucl. Data Tables* **42**, 189 (1989).
- [24] I. Berkes, M. De Jesús, B. Hlimi, M. Massa, E. H. Sayouty, and K. Heyde, *Phys. Rev. C* **44**, 104 (1991).
- [25] S. Raman, C. W. Nestor, Jr., and P. Tikkanen, *At. Data Nucl. Data Tables* **78**, 1 (2001).
- [26] J. Holden, N. Benczer-Koller, G. Jakob, G. Kumbartzki, T. J. Mertzimekis, K.-H. Speidel, A. Macchiavelli, M. McMahan, L. Phair, P. Maier-Komor, A. E. Stuchbery, W. F. Rogers, and A. D. Davies, *Phys. Lett. B* **493**, 7 (2000).
- [27] J. Holden, N. Benczer-Koller, G. Jakob, G. Kumbartzki, T. J. Mertzimekis, K.-H. Speidel, C. W. Beausang, R. Krücken, A. Macchiavelli, M. McMahan, L. Phair, A. E. Stuchbery, P. Maier-Komor, W. F. Rogers, and A. D. Davies, *Phys. Rev. C* **63**, 024315 (2001).
- [28] G. Jakob, N. Benczer-Koller, G. Kumbartzki, J. Holden, T. J. Mertzimekis, K.-H. Speidel, R. Ernst, A. E. Stuchbery, A. Pakou, P. Maier-Komor, A. Macchiavelli, M. McMahan, L. Phair, and I. Y. Lee, *Phys. Rev. C* **65**, 024316 (2002).
- [29] M. J. Taylor, N. Benczer-Koller, G. Kumbartzki, T. J. Mertzimekis, S. J. Q. Robinson, Y. Y. Sharon, L. Zamick, A. E. Stuchbery, C. Hutter, C. W. Beausang, J. J. Ressler, and M. A. Caprio, *Phys. Lett. B* **559**, 187 (2003).
- [30] G. D. Dracoulis, F. Riess, A. E. Stuchbery, R. A. Bark, S. L. Gupta, A. M. Baxter, and M. Kruse, *Nucl. Phys.* **A493**, 145 (1989).
- [31] A. Bohr and B. R. Mottelson, *Nuclear Structure* (Benjamin, Reading, MA, 1975), Vol. II.
- [32] H. P. Blok, W. R. Zimmerman, J. J. Kraushaar, and P. A. Batay-Csorba, *Nucl. Phys.* **A287**, 156 (1977).
- [33] O. A. Rosso, W. Unkelbach, and G. Molnár, *Nucl. Phys.* **A563**, 74 (1993).
- [34] H. Ohm, M. Lang, G. Molnar, S. Raman, K. Sistemich, and W. Unkelbach, *Phys. Lett. B* **241**, 472 (1990).
- [35] R. H. Spear, *At. Data Nucl. Data Tables* **42**, 55 (1989).